

ON THE GEOMETRY OF VIRTUAL KNOTS

by

Rachel Elizabeth Byrd

A thesis

submitted in partial fulfillment

of the requirements for the degree of

Master of Science in Mathematics

Boise State University

May 2012

© 2012
Rachel Elizabeth Byrd
ALL RIGHTS RESERVED

BOISE STATE UNIVERSITY GRADUATE COLLEGE

DEFENSE COMMITTEE AND FINAL READING APPROVALS

of the thesis submitted by

Rachel Elizabeth Byrd

Thesis Title: On the Geometry of Virtual Knots

Date of Final Oral Examination: 01 March 2012

The following individuals read and discussed the thesis submitted by student Rachel Elizabeth Byrd, and they evaluated her presentation and response to questions during the final oral examination. They found that the student passed the final oral examination.

Jens Harlander, Ph.D.

Chair, Supervisory Committee

Andrés Caicedo, Ph.D.

Member, Supervisory Committee

Uwe Kaiser, Ph.D.

Member, Supervisory Committee

The final reading approval of the thesis was granted by Jens Harlander, Ph.D., Chair, Supervisory Committee. The thesis was approved for the Graduate College by John R. Pelton, Ph.D., Dean of the Graduate College.

ABSTRACT

The Dehn complex of prime, alternating virtual links has been shown to be non-positively curved in the paper “Generalized knot complements and some aspherical ribbon disc complements” by J. Harlander and S. Rosebrock (2003) [7]. This thesis investigates the geometry of an arbitrary alternating virtual link. A method is constructed for which the Dehn complex of any alternating virtual link may be decomposed into Dehn complexes with non-positive curvature. We further study the relationship between the Dehn space and Wirtinger space, and we relate their fundamental groups using generating curves on surfaces. We conclude with interesting examples of Dehn complexes of virtual link diagrams, which illustrate our findings.

TABLE OF CONTENTS

| | |
|--|-----|
| ABSTRACT | iv |
| LIST OF FIGURES | vii |
| 1 INTRODUCTION | 1 |
| 2 THE DEHN COMPLEX OF A VIRTUAL KNOT | 4 |
| 2.1 The Virtual Knot and Various Complements | 4 |
| 2.2 Link Graphs of the Dehn Complex | 10 |
| 2.3 Reducing Circles | 13 |
| 2.4 Checkerboard Colorings and Closed Curves | 15 |
| 3 NON-POSITIVE CURVATURE OF THE DEHN COMPLEX ... | 21 |
| 3.1 Non-Positive Curvature | 21 |
| 3.2 Closed Curves in the Dehn Complex | 23 |
| 3.3 Decomposition of the Dehn Complex | 29 |
| 3.4 Tripling a Virtual Knot | 34 |
| 4 VIRTUAL KNOT DIAGRAMS AND LABELED | |
| ORIENTED GRAPHS | 37 |
| 4.1 Labeled Oriented Graphs | 37 |
| 4.2 Virtual Knots with Trivial Dehn Group | 38 |
| 4.3 Examples of Decompositions of the Dehn Complex | 41 |

| | |
|---|----|
| 5 ASPHERICITY OF VIRTUAL KNOTS | 47 |
| 5.1 Classical Closed Knot | 48 |
| 5.2 Virtual Closed Knot | 48 |
| 5.3 Virtual Long Knot | 49 |
| REFERENCES | 51 |

LIST OF FIGURES

| | | |
|------|--|----|
| 2.1 | A usual crossing and a virtual crossing. | 4 |
| 2.2 | The construction of the projection surface of a virtual knot diagram. (This is an imitation of the original image found in Kauffman [12].) . . . | 5 |
| 2.3 | A crossing of a knot with connected components labeled and the corresponding boundary of a 2-cell in the Dehn complex. | 7 |
| 2.4 | The Wirtinger relation $a_i a_j = a_j a_k$ given by a crossing of a virtual knot diagram. | 8 |
| 2.5 | (The “virtual trefoil”). The connected components of the Dehn complex of the virtual knot diagram are labeled A_1 and A_2 , and an orientation of the diagram is indicated with the generators of the Wirtinger complex, labeled a_1 and a_2 | 8 |
| 2.6 | The 1-skeleton and 2-cells of the Dehn complex of the virtual knot diagram in Figure 2.5. | 9 |
| 2.7 | The red arcs in the 2-cell (left side) indicate the edges that this 2-cell contributes to the v_+ link graph (right side) of the Dehn complex. . . . | 10 |
| 2.8 | Example of a reducing circle (the blue circle) on a 2-sphere and also a separating reducing circle (the blue circle) on a double torus. | 13 |
| 2.9 | A reducing circle lying on a portion of a virtual knot diagram. | 14 |
| 2.10 | An alternating virtual knot diagram (see Example 3.2.4) on a projection surface, the torus, with a checkerboard coloring. | 15 |

| | | |
|------|---|----|
| 2.11 | A portion of an alternating virtual link diagram with a non-separating reducing circle on a torus projection surface, and the resulting projection surface (the 2-sphere) after cutting along the reducing circle. Note that “ o ” stands for an over-crossing label and that “ u ” stands for an under-crossing label. | 18 |
| 3.1 | An alternating virtual knot diagram with a torus projection surface obtained by identifying the indicated edges in the figure. | 22 |
| 3.2 | The two possible orientations of non-separating reducing circles, N^- and N^+ | 24 |
| 3.3 | The slice of $\mathcal{M}(\ell)$ made along the non-separating reducing circles, for the N^- case and the N^+ case. | 25 |
| 3.4 | A continuous deformation of the twice punctured 2-sphere. We collapse all the 2-cell material by pushing in the boundary components y_1 and y_2 | 25 |
| 3.5 | A fully labeled and oriented alternating virtual knot diagram with three crossings. The dashed red line represents a non-separating reducing circle. (Virtual knot number 3.7 from Green and Bar-Natan [6].) | 28 |
| 3.6 | A double torus with a separating reducing circle indicated. | 30 |
| 3.7 | $\mathcal{M}(\ell_1)$ and $\mathcal{M}(\ell_2)$ obtained from $\mathcal{M}(\ell)$ | 31 |
| 3.8 | A non-separating reducing circle on a handle of the projection surface of the virtual link ℓ and the resulting cut surface and virtual link ℓ' | 32 |
| 3.9 | An alternating triple of an alternating virtual knot diagram (Example 3.2.4). | 34 |

| | | |
|------|---|----|
| 3.10 | A portion of the alternating virtual link diagram ℓ (black strands) and the additional links from tripling ℓ (red strands). The new strands are chosen to alternate with the original strands. | 35 |
| 3.11 | The remaining crossings of ℓ_T are chosen to alternate with the existing crossings. | 35 |
| 4.1 | A single edge of a LOG and the knot diagram crossing associated to that edge. The edge of the LOG gives the Wirtinger relation $a_i a_j = a_j a_k$. 37 | |
| 4.2 | An alternating virtual knot diagram with one non-separating reducing circle, indicated by the red line, obtained by identifying the labeled edges. | 41 |
| 4.3 | The alternating virtual link diagram of Figure 4.2 with the reducing circle cut out. The new prime knot is planar. | 42 |
| 4.4 | A labeled and oriented alternating virtual knot diagram with a non-separating reducing circle indicated by the red dashed line. On the right side is the corresponding LOC. (Virtual Knot number 4.105 from Green and Bar-Natan [6].) | 43 |
| 4.5 | The resulting virtual knot diagram k' and its corresponding LOCs after cutting along the non-separating reducing circle indicated in Figure 4.4. The dashed red lines indicate separating reducing circles. | 44 |
| 4.6 | The resulting virtual link diagram of k'_1 , k'_2 , and k'_3 and their corresponding LOCs after cutting along the separating reducing circles indicated in Figure 4.5. | 45 |

CHAPTER 1

INTRODUCTION

The topological and geometric aspects of classical knot complements have been intensely studied. First results related to this thesis include work by Aumann [2], who used combinatorial topological techniques on the Dehn complex to show the asphericity of alternating knots, and work by Weinbaum [16], who studied knot complements in terms of small cancellation theory. Modern treatments of the curvature of knot complements have been given by D. T. Wise [18] in terms of non-positively curved squared complexes, and this viewpoint was developed by Bridson and Haefliger [4].

This thesis investigates the topological and geometric aspects of the Dehn complex of a virtual knot. We are particularly interested in when a virtual knot admits a Dehn complex that is a non-positively curved squared complex. There are various descriptions of the fundamental group of the Dehn complex. One is obtained by collapsing an edge in the Dehn complex, and the other is obtained by coning off a surface in the Wirtinger complex. All these descriptions can be read off the virtual knot drawn on its projection surface.

The Dehn groups and the Wirtinger groups of classical knots have properties that are not present in Dehn groups of virtual knots. A simple example is the “virtual trefoil” (see Example 2.1.5 for details). The presentation of the Wirtinger group of the virtual trefoil,

$$\langle a_1, a_2 \mid a_1 a_1 = a_1 a_2, a_2 a_1 = a_1 a_1 \rangle$$

is infinite cycle, which is not unusual. However, the presentation of the Dehn group of the virtual trefoil,

$$\langle A_1, A_2 \mid A_1 = 1, A_2 A_2^{-1} A_2 A_1^{-1} = 1, A_2 A_2^{-1} A_2 A_1^{-1} = 1 \rangle$$

is the trivial group. Dehn groups that are trivial or that have torsion do not occur in the classical case. We will illustrate the exotic behavior of Dehn groups with further examples later.

Using the close relationship between the Wirtinger complex and the Dehn complex, we use curves on the surface of the Wirtinger space to obtain the Dehn group from the Wirtinger group.

Theorem (Main Theorem I). *The fundamental group of the Dehn complex $\pi_1(D(\ell))$ is isomorphic to the quotient $\pi_1(W(\ell)) / K$, where K is normally generated by words $y_1^{\epsilon_1} y_2^{\epsilon_2} \cdots y_n^{\epsilon_n}$ that arise when reading along the curves that generate the fundamental group of the projection surface F .*

Consider the following result of Bridson and Haefliger [4, p. 220], included in their treatment of the Dehn complex of the classical knot complement.

Theorem (Bridson/Haefliger [4]). *If $\mathcal{K} \subset \mathbb{R}^3$ is an alternating link then $\pi_1(\mathbb{R}^3 - \mathcal{K})$ is the fundamental group of a compact 2-dimensional piecewise-Euclidean 2-complex of non-positive curvature.*

Harlander and Rosebrock [7] extended this result to prime alternating virtual links. They used a strong version of primeness.

Theorem (Harlander/Rosebrock [7]). *A virtual link diagram ℓ is prime, alternating if and only if the Dehn complex of ℓ is a non-positively curved squared complex.*

In this thesis, we study arbitrary alternating virtual links. The existence of torsion in the Dehn groups presents obstacles in obtaining a result identical to the classical one. Our result is a method for decomposing the Dehn complex of an alternating virtual link into non-positively curved squared complexes.

Theorem (Main Theorem II). *If ℓ is an alternating virtual link diagram drawn on a projection surface F , then we can cut along a finite number of reducing circles to obtain a collection of prime, alternating links, ℓ_1, \dots, ℓ_n . This gives a decomposition of the Dehn complex of ℓ , $D(\ell)$, into non-positively curved squared complexes, and a decomposition of the fundamental group of $D(\ell)$ into $CAT(0)$ groups.*

We conclude with examples of virtual knots with various reducing circles to illustrate the method of Main Theorem II.

CHAPTER 2

THE DEHN COMPLEX OF A VIRTUAL KNOT

2.1 The Virtual Knot and Various Complements

Virtual knots and links are an extension of classical knot theory and were first introduced by Kauffman [13].

Definition 2.1.1 (Virtual Link Diagrams). A virtual link diagram ℓ is a 4-regular graph in the plane, with over-crossing and under-crossing information at some nodes. The nodes with this additional information are crossings, and the remaining nodes are called virtual crossings. The latter are indicated by a circle around the node. From a virtual link diagram in the plane, we construct a closed, orientable surface

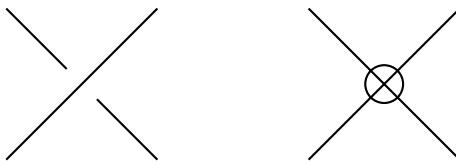


Figure 2.1: A usual crossing and a virtual crossing.

F of minimal genus in which ℓ embeds, so that only crossings appear as nodes. The virtual crossings disappear because we can run the edges of the graph over handles. The details of this construction are as follows. Start with the graph and embed it in \mathbb{R}^3 so that the virtual crossings disappear. We obtain a 2-manifold with boundary by thickening every edge of the graph into a band. For every boundary component,

glue in a disc to obtain the desired surface. We call the surface thus obtained the projection surface F of ℓ (see Figure 2.2).

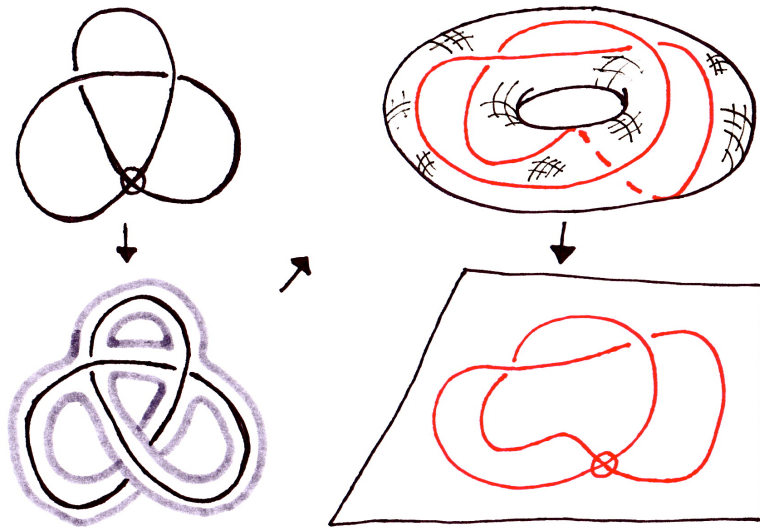


Figure 2.2: The construction of the projection surface of a virtual knot diagram. (This is an imitation of the original image found in Kauffman [12].)

Definition 2.1.2 (Various Virtual Link Complements). Given a virtual link diagram ℓ , let F be a projection surface. We can push the diagram into the interior of the thickened surface $F \times I$, and thus obtain an embedding of circles in $F \times I$. We denote the image of this embedding by $\hat{\ell}$. If we remove an open neighborhood of $\hat{\ell}$ from $F \times I$, then we obtain a compact manifold with boundary, which we will call the manifold space, $\mathcal{M}(\ell)$. If we cone off the bottom surface $F \times \{0\}$ of $\mathcal{M}(\ell)$, we obtain a compact pseudomanifold with boundary, which we call the Wirtinger space, $\mathcal{W}(\ell)$. It turns out that $\mathcal{W}(\ell)$ can be collapsed to the 2-dimensional Wirtinger complex, $W(\ell)$. If we cone off the top surface in the Wirtinger space, we obtain another compact pseudomanifold with boundary, which we call the Dehn space, $\mathcal{D}(\ell)$. The Dehn space can be collapsed down to the 2-dimensional Dehn complex, $D(\ell)$. See Harlander and

Rosebrock [7] for details on this collapsing procedure on the Wirtinger space and the Dehn space.

We will now give detailed descriptions of the cell structure of these various complements.

Definition 2.1.3 (Dehn Complex). There are two vertices, v_+ and v_- , which are the cone points. The edges are in 1-1 correspondence with the connected components, A_1, A_2, \dots, A_n , of $F - \ell$. Each edge A_i is oriented from v_+ to v_- . The connected components of a classical knot are simply the connected components of $\mathbb{R}^2 - \ell$, since ℓ is a planar graph. However, for a non-planar virtual link diagram, we have to take the virtual crossings into consideration. To find the connected component A_i , follow along on a particular side of any edge in the virtual link diagram. If we encounter a crossing, label that quadrant of the crossing as A_i and turn at the crossing to stay within the A_i component. If we encounter a virtual crossing, it is not an actual crossing. Thus, we continue straight through the virtual crossing without turning or labeling. We can continue in this fashion until we have found each connected component and hence labeled every quadrant of each crossing of ℓ . The faces are in 1-1 correspondence with the crossings of ℓ . Considering a particular crossing of ℓ : proceed counterclockwise around the crossing $x \in \ell$, starting at the end of an edge of ℓ that is an over-crossing, and read off the four (not necessarily distinct) components encountered, say $A_{x(1)}, A_{x(2)}, A_{x(3)}$, and $A_{x(4)}$. A 2-cell is attached to the edge-path, $A_{x(1)}A_{x(2)}^{-1}A_{x(3)}A_{x(4)}^{-1}$ (see Figure 2.3).

Without loss of generality, we may choose the tree of the 1-skeleton of $D(\ell)$ to be the edge A_1 . If we collapse the tree to a point, choosing it to be our basepoint d_0 , we can write down the canonical presentation of $\pi_1(D(\ell), d_0)$, the Dehn group, from the

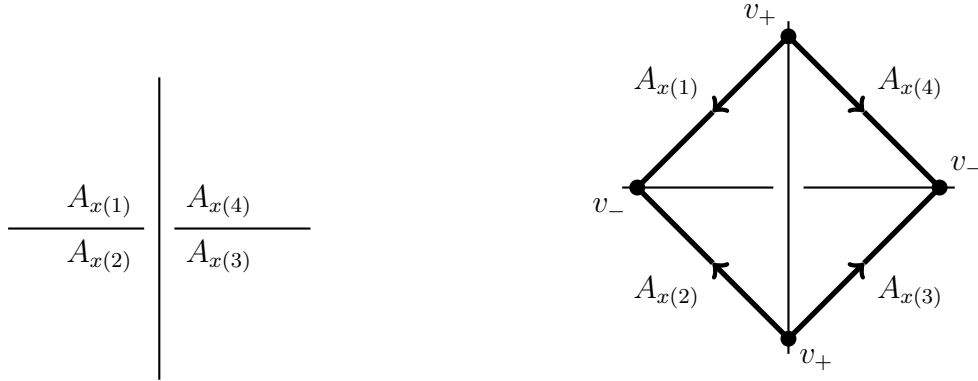


Figure 2.3: A crossing of a knot with connected components labeled and the corresponding boundary of a 2-cell in the Dehn complex.

edges (the generators) A_1, \dots, A_n and from the faces (the relations) with boundaries read-off from ℓ (see Hog-Angeloni and Metzler [10]).

$$\pi_1(D(\ell)) = \langle A_1, A_2, A_3, \dots, A_n \mid A_1 = 1, \quad A_{x(1)} A_{x(2)}^{-1} A_{x(3)} A_{x(4)}^{-1} = 1 \\ \text{for every crossing } x \in \ell \rangle$$

Definition 2.1.4 (Wirtinger Complex). The edges of any virtual link diagram ℓ may be oriented, and each un-broken edge of the link diagram—the edge encounters no under-crossings—may be labeled from the set, $\{a_1, a_2, \dots, a_n\}$. These are the generators of the fundamental group of the Wirtinger complex. The faces are in one-to-one correspondence with the crossings of ℓ . Using the “right hand rule,” we can orient the boundary of the faces based upon the orientation of the edges corresponding to a particular crossing in the virtual link diagram, as done in Figure 2.4. There is only one vertex in the Wirtinger complex—the cone point—which we choose as our basepoint, w_0 . We can now write down the canonical presentation of the fundamental group of the Wirtinger complex, the Wirtinger group.

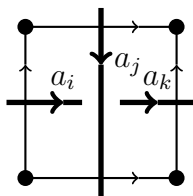


Figure 2.4: The Wirtinger relation $a_i a_j = a_j a_k$ given by a crossing of a virtual knot diagram.

$$\pi_1(W(\ell)) = \langle a_1, a_2, \dots, a_n \mid R_1, \dots, R_m \rangle$$

where every relation, R_i , is of the form $a_i a_j = a_j a_k$, corresponding to a crossing in the virtual knot diagram.

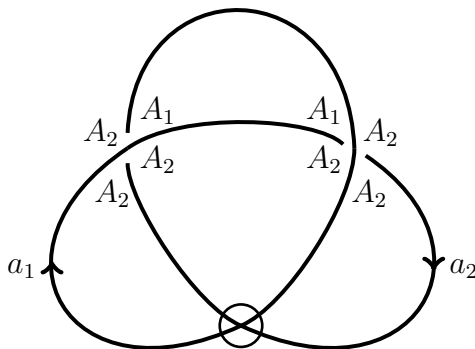


Figure 2.5: (The “virtual trefoil”). The connected components of the Dehn complex of the virtual knot diagram are labeled A_1 and A_2 , and an orientation of the diagram is indicated with the generators of the Wirtinger complex, labeled a_1 and a_2 .

Example 2.1.5 (Virtual knot with $\pi_1(D(k))$ trivial). Consider the virtual knot diagram, k , with two crossings, in Figure 2.5. We have labeled the connected components of the projection surface, and an orientation has been given to the edges, in order to label the Wirtinger generators. The projection surface is a torus, as seen in Figure

2.2. We also can count the Euler characteristic of the projection surface by using the virtual knot diagram in Figure 2.5 and obtain, $\chi = 2 - 4 + 2 = 0$.

We have the following presentation of the Dehn group given by k , where the labeling is defined in Figure 2.5. The 2-cells corresponding to each crossing are drawn in Figure 2.6. We perform Tietze transformations to simplify the group presentation (see Hog-Angeloni and Metzler [10]).

$$\begin{aligned} \pi_1(D(k)) &= \langle A_1, A_2 \mid A_1 = 1, A_2 A_2^{-1} A_2 A_1^{-1} = 1, A_2 A_2^{-1} A_2 A_1^{-1} = 1 \rangle \\ &\approx \langle A_1, A_2 \mid A_1 = 1, A_2 = A_1 \rangle \\ &\approx \langle A_1 \mid A_1 = 1 \rangle \\ &\approx \{1\} \end{aligned}$$

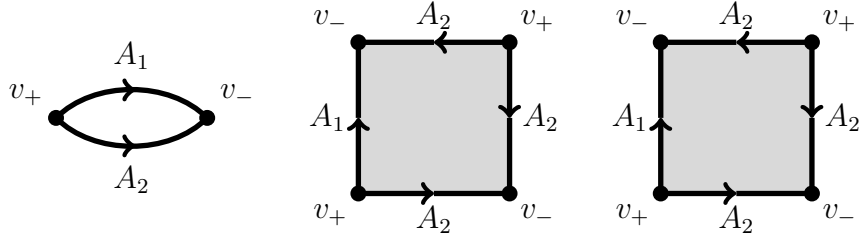


Figure 2.6: The 1-skeleton and 2-cells of the Dehn complex of the virtual knot diagram in Figure 2.5.

We also have the following presentation of the Wirtinger group given the orientation of the edges of the virtual knot diagram.

$$\begin{aligned} \pi_1(W(k)) &= \langle a_1, a_2 \mid a_1 a_1 = a_1 a_2, a_2 a_1 = a_1 a_1 \rangle \\ &\approx \langle a_1 \rangle \\ &\approx \mathbb{Z} \end{aligned}$$

We observe that the Wirtinger group is infinite cyclic, while the Dehn group is trivial $\{1\}$.

As the preceding example shows, the Dehn complex of virtual link diagrams can frequently produce unusual fundamental groups such as the trivial group or groups with torsion, which cannot occur with the Wirtinger complex.

2.2 Link Graphs of the Dehn Complex

The link graph (or Whitehead graph) of a complex describes the local curvature of the complex (see Bridson and Haefliger [4]). This geometric approach can be useful over using a metric approach. We will use the link graphs later to define non-positive curvature in a squared 2-complex (Definition 3.1.1).

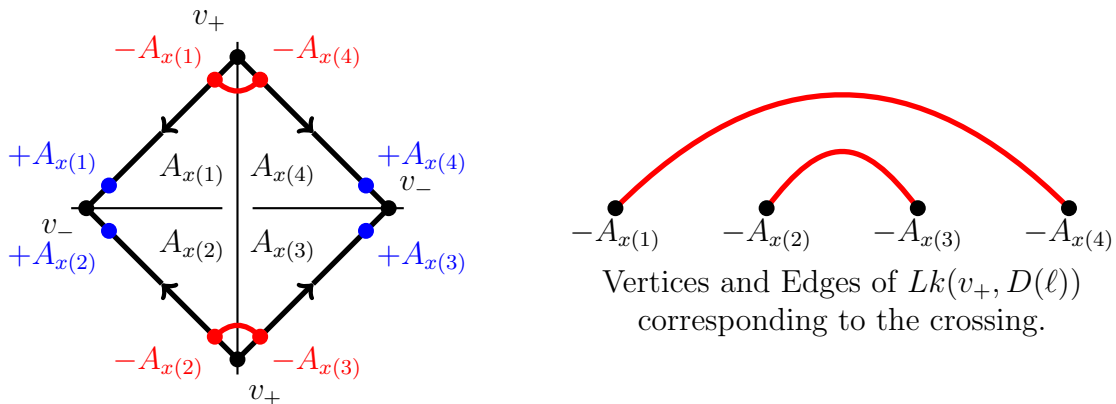


Figure 2.7: The red arcs in the 2-cell (left side) indicate the edges that this 2-cell contributes to the v_+ link graph (right side) of the Dehn complex.

Definition 2.2.1 (Link Graphs). The link graph of a vertex of the Dehn complex of a virtual link diagram ℓ is the boundary of a neighborhood of that vertex in the 2-dimensional Dehn complex. Denote the link graph of, say v_+ of $D(\ell)$, by

$Lk(v_+, D(\ell))$. Each edge, A_i , in the 2-complex contributes a $+A_i$ vertex and a $-A_i$ vertex to the link graph. However, by virtue of the consistent orientation of each edge in $D(\ell)$ (each edge is oriented v_+ to v_-), for each end of an edge that is an over-crossing, there is one edge in $Lk(v_+, D(\ell))$ connecting the $-$ vertices with the labels of the adjacent connected components of that edge. The $+$ vertices are not used in $Lk(v_+, D(\ell))$. In parallel, for each end of an edge in ℓ that is an under-crossing, there is a single edge in $Lk(v_-, D(\ell))$ that connects the $+$ vertices with the labels of the adjacent connected components of that edge. This is all shown, for one 2-cell of $D(\ell)$ for $Lk(v_+, D(\ell))$, in Figure 2.7.

Definition 2.2.2 (Dual Tessellation). Let F be a projection surface constructed from a virtual link diagram ℓ as in Definition 2.1.1. Denote the 1-skeleton of F also by ℓ (slight abuse of notation). The dual tessellation is constructed by placing a vertex in each connected component, A_0, A_1, \dots, A_n , of $F - \ell$. Every edge of ℓ has a connected component on either side, forming a pair, say (A_i, A_j) . In the dual, we connect the pair of vertices, (A_i, A_j) , with an edge that transversally intersects that edge of ℓ between the pair (A_i, A_j) . We remark that the vertices of the dual are in 1-1 correspondence with the connected components of $F - \ell$ and that the edges of the dual are in 1-1 correspondence with the edges of ℓ .

Proposition 2.2.3. *Let ℓ be an alternating virtual link diagram with a projection surface F . Then, the graphs $Lk(v_+, D(\ell)) = Lk(v_-, D(\ell)) = X$, where X is the 1-skeleton of the dual tessellation of the projection surface F .*

Proof. The connected components, the edges of $D(\ell)$, are in 1-1 correspondence with the vertex sets of $Lk(v_+, D(\ell))$ and $Lk(v_-, D(\ell))$, as we stated in the Definition 2.2.1. Since ℓ is alternating, each edge has one end labeled an over-crossing and the

other labeled an under-crossing. For each edge, there is a pair (A_i, A_j) of connected components that abut either side of the edge. Consequently, each edge with pair (A_i, A_j) contributes one edge connecting vertices $-A_i$ and $-A_j$ in $Lk(v_+, D(\ell))$ and one edge connecting vertices $+A_i$ and $+A_j$ in $Lk(v_-, D(\ell))$. Hence, the edges of the virtual link diagram ℓ are in 1-1 correspondence with the edges of each link graph. Thus, $Lk(v_+, D(\ell)) = Lk(v_-, D(\ell))$.

In the dual tessellation X , there is a vertex for each connected component of $F - \ell$, as there is for $Lk(v_+, D(\ell))$ and $Lk(v_-, D(\ell))$. Each edge in ℓ contributes an edge to X connecting the vertices with the labels of the adjacent connected components, as there is for $Lk(v_+, D(\ell))$ and $Lk(v_-, D(\ell))$. Therefore, the vertex set and edge set of X , $Lk(v_+, D(\ell))$, and $Lk(v_-, D(\ell))$ are equivalent. \square

For the alternating case, we will use the notation, $Lk(v_{\pm}, D(\ell))$, to indicate either $Lk(v_+, D(\ell))$ or $Lk(v_-, D(\ell))$ works, since the graphs are equivalent.

Lemma 2.2.4. *If a virtual link diagram ℓ is not alternating, then there is at least one 2-cycle in the link graphs of ℓ .*

Proof. If the virtual link diagram ℓ is not alternating, then ℓ has at least one edge, say y , whose ends have the same label. Suppose the pair of connected components (A_i, A_j) abut along the edge y . For non-alternating, we may assume that the ends of y are both labeled as over-crossings. Hence, y contributes two edges to $Lk(v_+, D(\ell))$, each connecting the vertex $-A_i$ to the vertex $-A_j$. These two edges form a 2-cycle in $Lk(v_+, D(\ell))$. \square

However, a 2-cycle in the link graphs does not imply that a virtual knot diagram is not alternating.

2.3 Reducing Circles

In this section, we will develop the definition of the strong version of primeness, as used by Harlander and Rosebrock [7]. On a surface of genus ≥ 1 , there exist closed curves on the surface that separate the surface and also closed curves that do not separate the surface (i.e. non-separating cut a handle open).

Definition 2.3.1 (Reducing Circle). Let ℓ be a virtual link diagram with a projection surface F . A simple, closed curve on F that intersects ℓ exactly twice is a reducing circle. When the reducing circle is separating, we require that crossings are contained on both sides of the separating reducing circle.

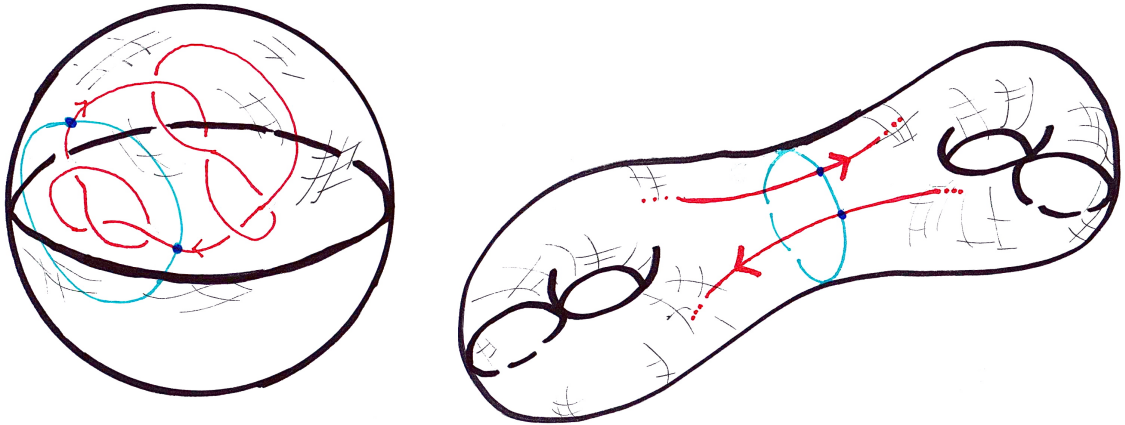


Figure 2.8: Example of a reducing circle (the blue circle) on a 2-sphere and also a separating reducing circle (the blue circle) on a double torus.

Separating reducing circles lead to decompositions of the link diagram. If we cut a virtual link diagram ℓ along a reducing circle and connect the four new endpoints with two new small arcs, we obtain two virtual link diagrams, ℓ_1 and ℓ_2 , and ℓ is called the composition of ℓ_1 and ℓ_2 , $\ell = \ell_1 \# \ell_2$ (see Adams [1], and Bridson and Haefliger [4]).

Cutting along a non-separating reducing circle also simplifies the virtual link diagram, and this often leads to a virtual link diagram whose projection surface is of smaller genus. However, this is not a decomposition as with separating reducing circles (for an example, see Figure 2.11).

Definition 2.3.2 (Prime Virtual Link). A virtual link diagram is prime if there are no reducing circles, separating or non-separating.

Lemma 2.3.3. *If a virtual link diagram ℓ is not prime, then there is at least one 2-cycle in the link graphs of ℓ .*

Proof. If the virtual link diagram ℓ is not prime, then ℓ admits a reducing circle. A separating or non-separating reducing circle does not signify. The reducing circle intersects ℓ transversally twice, say along the edges y_1 and y_2 in ℓ . The reducing circle lies in the connected components that abut along y_1 and y_2 , say the pair, (A_i, A_j) , as we diagram in Figure 2.9. The edges, y_1 and y_2 , are distinct since we defined

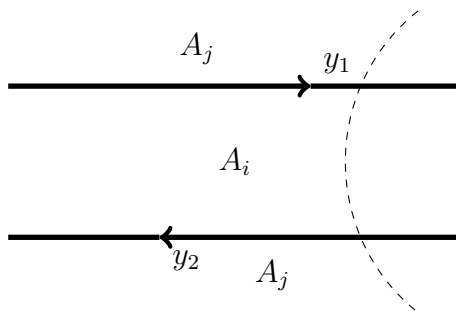


Figure 2.9: A reducing circle lying on a portion of a virtual knot diagram.

the reducing circle to not be trivial. If ℓ is alternating, then y_1 and y_2 with both contribute one edge, each, to $Lk(v_+, D(\ell))$, connecting the vertex $-A_i$ to the vertex $-A_j$, a 2-cycle. If ℓ is not alternating, y_1 and y_2 may still have one end labeled as an over-crossing and the other as an under-crossing, in which case we are in the

alternating situation. If either y_1 or y_2 have both ends with the same label, without loss of generality, say y_1 has both ends labeled as an over-crossing, then y_1 contributes a 2-cycle connecting the vertices $-A_i$ and $-A_j$ in $Lk(v_+, D(\ell))$. \square

However, 2-cycles in the link graphs do not imply that a virtual link is not prime. A 2-cycle may indicate non-alternating.

2.4 Checkerboard Colorings and Closed Curves

A tessellated orientable surface has a checkerboard coloring if the faces can be colored alternately black or white so that every edge bounds faces of different color. For an example, see Figure 2.10.

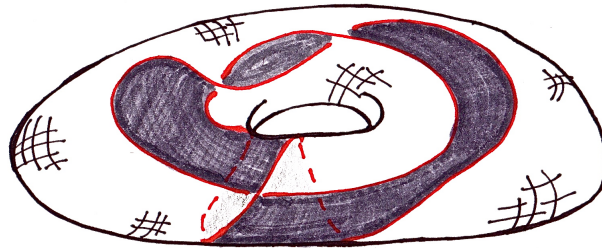


Figure 2.10: An alternating virtual knot diagram (see Example 3.2.4) on a projection surface, the torus, with a checkerboard coloring.

Theorem 2.4.1 (Kamada [11]). *The projection surface of an alternating virtual link diagram has a checkerboard coloring.*

Following the convention used by Bridson and Haefliger [4, p 223] for coloring the connected components alternately black or white: let ℓ be an alternating virtual link diagram with a projection surface F . For each connected component of $F - \ell$, each edge that lies on the boundary of a connected component has one end labeled

as an over-crossing and the other end labeled as an under-crossing. Hence, the closed edge-path that makes up the boundary of each connected component has a consistent orientation of the crossing labels on each edge. We will label a connected component “white” if all the edges bounding the component are labeled as an under-crossing end to an over-crossing end when we trace the boundary in a counterclockwise fashion. Conversely, we will label a connected component “black” if instead the edges are labeled as an over-crossing end to an under-crossing end, counterclockwise. Any edge on the boundary of a connected component that runs around the outermost position of the virtual link diagram (lying on the plane) is colored in an opposite fashion to the convention stated. The boundary of a connected component may run along the outermost position and also the inner positions of the diagram.

Proposition 2.4.2. *Given an alternating virtual link diagram ℓ with a projection surface F , then any closed curve intersects ℓ at an even number of points.*

Proof. The connected components of $F - \ell$ has a checkerboard coloring (Theorem 2.4.1). Each time a closed curve intersects ℓ (this is a transversal intersection, not at a crossing of ℓ) the curve passes from one colored component to a different colored component, say black to white. Hence, any closed curve runs through $2n$ components and intersects ℓ $2n$ times, for some $n \in \mathbb{N}$. □

Lemma 2.4.3. *Given an alternating virtual link diagram ℓ with a projection surface F : there exists a closed curve in F that intersects ℓ n times if and only if there exists an edge cycle in $Lk(v_{\pm}, D(\ell))$ of n edges. In particular, $Lk(v_{\pm}, D(\ell))$ contains cycles only of even length.*

Proof. We may just consider $Lk(v_+, D(\ell))$ in the proof since $Lk(v_+, D(\ell)) = Lk(v_-, D(\ell))$ for ℓ alternating (Proposition 2.2.3).

Suppose a closed curve intersects ℓ on its projection surface F n times. By Proposition 2.4.2, n is even. Let $\{y_1, \dots, y_n\}$ be the set of edges of ℓ that the closed curve transversally intersects. For ease of notation, let the pair of connected components on either side of edge y_i be the pair (A_i, A_{i+1}) . Using that ℓ is alternating, y_i contributes an edge connecting vertices $-A_i$ and $-A_{i+1}$ in $Lk(v_+, D(\ell))$. Hence, we have an edge cycle of n edges connecting vertices $-A_1$ to $-A_2, \dots, -A_{n-1}$ to $-A_n$, and $-A_n$ to $-A_1$ in $Lk(v_+, D(\ell))$.

For an edge path in $Lk(v_+, D(\ell))$ that connects vertices $-A_1$ to $-A_2, \dots, -A_{n-1}$ to $-A_n$, and $-A_n$ to $-A_1$, each edge is contributed because of an edge y_i in ℓ that has the pair of connected components (A_i, A_{i+1}) on either side. Hence, there is a closed curve on F that runs through the connected components A_1, A_2, \dots, A_n and intersects the edges y_1, y_2, \dots, y_n of ℓ on F . By Proposition 2.4.2, n must be an even number. \square

In particular, we have shown that any closed curve on F corresponds to an edge path in X .

Lemma 2.4.4. *A cut along any reducing circle on an alternating virtual link diagram yields an alternating virtual link diagram(s).*

Proof. Suppose ℓ is an alternating virtual link diagram with a non-trivial reducing circle. As shown in Figure 2.11, the reducing circle lies in two distinct connected components, say A_i and A_j . Since ℓ has a checkerboard coloring, we may assume that A_i is “white”, i.e. the edges forming the boundary are oriented under-crossing to over-crossing in a counterclockwise orientation around the boundary. This forces the labeling of the top edge, in Figure 2.11, to be over-crossing to under-crossing and the bottom edge to be under-crossing to over-crossing, when we read the labels

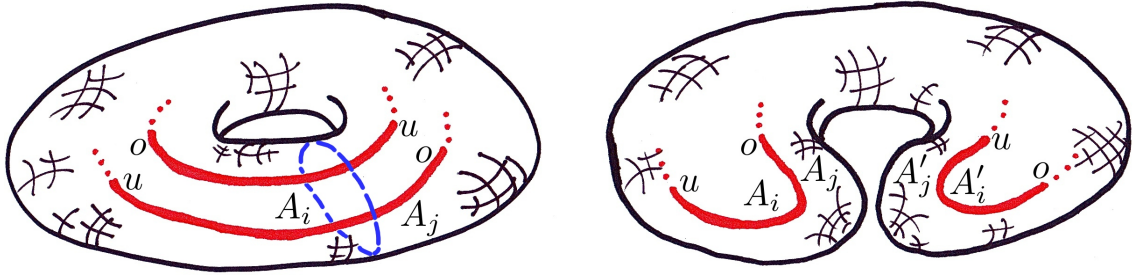


Figure 2.11: A portion of an alternating virtual link diagram with a non-separating reducing circle on a torus projection surface, and the resulting projection surface (the 2-sphere) after cutting along the reducing circle. Note that “ o ” stands for an over-crossing label and that “ u ” stands for an under-crossing label.

left-to-right, respectively. After we cut along the reducing circle and connect the new endpoints with new small arcs, the left-hand-side edge is alternating and the right-hand-side edge is alternating. Since we did not alter any of the over-crossings or under-crossings, nor did we alter any edges besides the two shown, the link, resulting from ℓ , is alternating. \square

Note that a cut along a separating reducing circle of a virtual link results in two new virtual links, while a cut along a non-separating reducing circle results in just one new virtual link.

Lemma 2.4.5. *For any alternating virtual link diagram ℓ , there are only finitely many reducing circles. Moreover, if we cut along a separating or non-separating reducing circle, the number of reducing circles decreases by at least one.*

Proof. For a given virtual link diagram ℓ with a projection surface F , we can use the graph of the dual tessellation to determine how many distinct reducing circles exist, up to isotopy. If there is a 2-cycle in the graph of the dual tessellation, then there are two connected components of $F - \ell$ that share two distinct edges of ℓ as in Figure 2.9. This admits a reducing circle corresponding to that 2-cycle in the dual tessellation.

Likewise, every reducing circle corresponds to a single 2-cycle in the graph of the dual tessellation. The dual tessellation is a finite graph. Hence, there are only a finite number of reduced 2-cycles in the dual tessellation that correspond to the number of reducing circles.

Suppose there is a reducing circle on F and the corresponding 2-cycle in the graph of the dual tessellation is two edges $\{y_1, y_2\}$ connecting the vertices A_i and A_j . When we cut and re-direct the edges of ℓ intersected by the reducing circle, we gain two components in the projection surface and hence two vertices $\{A'_i, A'_j\}$ in the graph of the dual tessellation. The vertices $\{A_i, A_j\}$ are connected by the edge y_1 and the vertices $\{A'_i, A'_j\}$ are connected by the edge y_2 . According to the nature of the cut on the particular surface, there is a partition of the edges connected to the vertex A_i between the new A_i and A'_i after the cut. The edges connected to A_j are also partitioned between the new A_j and A'_j after the cut.

There have been no additional edges added, nor have we changed any part of the graph except sharing the edges ending at the vertices A_i and A_j with the new vertices A'_i and A'_j and altering the edges y_1 and y_2 . Hence, we have decreased the number of 2-cycles by at least 1. \square

Lemma 2.4.6. *Every alternating virtual link diagram ℓ is a composition of finitely many links, each of which is alternating with no separating reducing circles.*

Proof. The alternating virtual link diagram ℓ with a projection surface F has only finitely many separating reducing circles (Lemma 2.4.5). If there are n separating reducing circles, then we have the composition of $(n + 1)$ virtual link diagrams,

$$\ell = \ell_0 \# \ell_1 \# \cdots \# \ell_n$$

where each virtual link diagram ℓ_i is alternating (Lemma 2.4.4). Each ℓ_i has no separating reducing circles, otherwise, ℓ on F would have had $(n + 1)$ separating reducing circles. Therefore, the only reducing circles each ℓ_i can possibly have are non-separating reducing circles. \square

CHAPTER 3

NON-POSITIVE CURVATURE OF THE DEHN COMPLEX

3.1 Non-Positive Curvature

A squared 2-complex is a complex where every 2-cell has four edges. The Dehn 2-complex and the Wirtinger 2-complex are examples of a squared 2-complex.

Definition 3.1.1 (Non-Positive Curvature). A squared 2-complex is non-positively curved if there are at least four squares grouped around each vertex. That is, if every reduced edge cycle in the link graph of each vertex in the 2-complex has length at least four.

We are now ready to prove Theorem 3.1.2 from Harlander and Rosebrock [7]. However, we do not give their proof of the theorem. The proof given follows from our development of virtual knots in the previous chapter.

Theorem 3.1.2 (Harlander/Rosebrock [7]). *A virtual link diagram ℓ is prime, alternating if and only if the Dehn complex of ℓ is a non-positively curved squared complex.*

Proof. Suppose that ℓ is alternating with a projection surface F . By Lemma 2.4.3, all edge cycles in $Lk(v_{\pm}, D(\ell))$ are of even length. We have a 2-cycle in $Lk(v_{\pm}, D(\ell))$ only if a pair of connected components of $F - \ell$, (A_i, A_j) , abut two distinct edges in ℓ .

However, we would be in the situation shown in Figure 2.9, which admits a reducing circle. Hence, $Lk(v_{\pm}, D(\ell))$ has cycles of even length greater than 2, and $D(\ell)$ is a non-positively curved squared complex (Definition 3.1.1).

If $D(\ell)$ is a non-positively curved squared complex, then all the cycles in the link graphs have length of at least four. By Lemma 2.2.4, ℓ admits a 2-cycle in the link graphs if it is not alternating, and by Lemma 2.3.3, ℓ also admits a 2-cycle in the link graphs if it is not prime. Therefore, ℓ is prime, alternating. \square

Example 3.1.3 (Classical links). Every classical link that is prime, alternating has a Dehn complex that is a non-positively curved squared complex.

Example 3.1.4 (Virtual knot with a non-positively curved Dehn complex). By identifying the indicated edges in Figure 3.1, we obtain an alternating virtual knot diagram on a torus. The Dehn complex of the virtual knot is non-positively curved as there are no reducing circles.

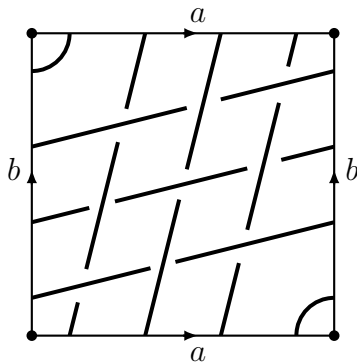


Figure 3.1: An alternating virtual knot diagram with a torus projection surface obtained by identifying the indicated edges in the figure.

3.2 Closed Curves in the Dehn Complex

Reducing circles present a barrier to obtaining a Dehn complex that is a non-positively curved squared complex. Consequently, we are interested in the relation a reducing circle forms in the fundamental group of $\mathcal{D}(\ell)$ and of $\mathcal{W}(\ell)$.

Since the Dehn space is obtained from the Wirtinger space by coning off the top surface (Definition 2.1.2), we have a quotient map $\varphi : \mathcal{W}(\ell) \rightarrow \mathcal{D}(\ell)$, which takes the basepoint $w_0 \in \mathcal{W}(\ell)$ to the basepoint $d_0 \in \mathcal{D}(\ell)$. The map φ induces a homomorphism between the fundamental groups of the 2-dimensional spines (the following arguments can be found in Hatcher [9]),

$$\varphi_* : \pi_1(W(\ell), w_0) \rightarrow \pi_1(D(\ell), d_0) \quad (3.1)$$

where φ_* is a mapping of composed loops $f : I \rightarrow \mathcal{W}(\ell)$ at the basepoint w_0 such that $\varphi_*[f] = [\varphi f]$. For any homotopy of loops $f_t : I \rightarrow \mathcal{W}(\ell)$ based at w_0 , we have that $\varphi_*[f_0] = [\varphi f_0] = [\varphi f_1] = \varphi_*[f_1]$. Hence, φ_* is well-defined. The map φ is a homomorphism since the composition of the loops $f, g : I \rightarrow \mathcal{W}(\ell)$ based at w_0 is:

$$f \cdot g = \begin{cases} f(2t), & 0 \leq t \leq 1/2 \\ g(2t - 1), & 1/2 \leq t \leq 1 \end{cases}$$

Hence, $\varphi(f \cdot g) = \varphi(f) \cdot \varphi(g)$, and it follows that φ_* is also a homomorphism. Since φ is quotient map, in the topological sense, Theorem 3.2.3 will use a van Kampen argument to show that φ_* is a surjection. In particular, $\pi_1(D(\ell))$ is a quotient of $\pi_1(W(\ell))$,

$$\pi_1(D(\ell)) \approx \pi_1(W(\ell)) / K$$

where the generators of K result from closed curves on $\mathcal{W}(\ell)$.

Suppose we place some consistent orientation on virtual link diagram ℓ . Any separating reducing circle on the projection surface of ℓ has opposing orientations on the edges of ℓ that are cut by the reducing circle (see Figure 2.8). However, the edges of ℓ cut by a non-separating reducing circle has two possible orientations, as shown in Figure 3.2. We will call them N^- reducing circles and N^+ reducing circles. Cutting along a N^- reducing circle changes the orientations of the virtual link diagram, while cutting along a N^+ reducing circle preserves the orientation of the virtual link diagram.

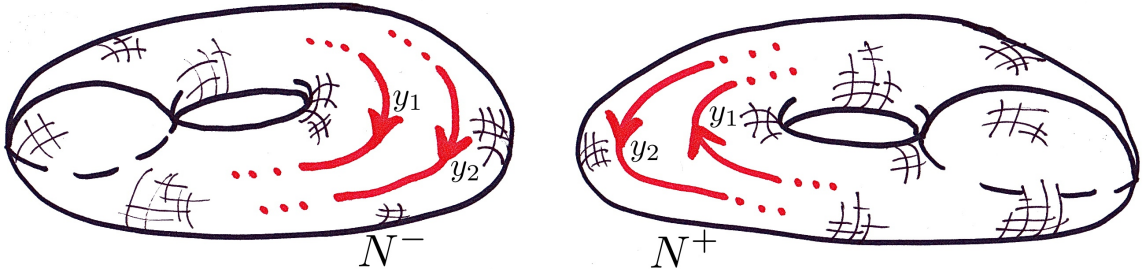


Figure 3.2: The two possible orientations of non-separating reducing circles, N^- and N^+ .

Proposition 3.2.1. *Using the notation of Figure 3.2 and Figure 3.3, and utilizing Equation 3.1. For separating or N^+ reducing circles, the relation $y_1 = y_2$ holds in $\pi_1(D(\ell))$ (i.e. $y_1 y_2^{-1} \in K$). For N^- reducing circles, $y_1 = y_2^{-1}$ in $\pi_1(D(\ell))$ (i.e. $y_1 y_2 \in K$).*

Proof. Suppose the virtual link diagram ℓ has a reducing circle, either separating or non-separating. Slice the manifold space, $\mathcal{M}(\ell)$, along the reducing circle. The slice made by the reducing circle is an annulus with two oriented punctures. Figure 3.3 shows how the orientations of the punctures, y_1 and y_2 , differ between the N^- case and the N^+ case.

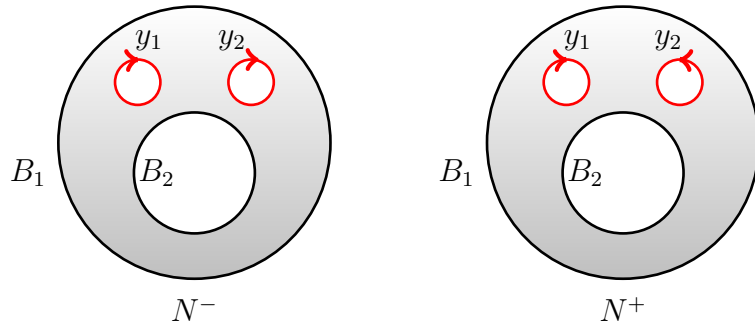


Figure 3.3: The slice of $\mathcal{M}(\ell)$ made along the non-separating reducing circles, for the N^- case and the N^+ case.

The top boundary, B_1 , and the bottom boundary, B_2 , of the slice are each coned off in the Dehn space, and the result is homeomorphic to a 2-sphere with two oriented punctures made by y_1 and y_2 . The 2-sphere with two punctures is homeomorphic to a circle, S^1 . Figure 3.4 shows, for a N^- non-separating reducing circle, how the orientations of the boundaries, y_1 and y_2 , are opposite on the cylinder. We can conclude that for a N^+ reducing circle, $y_1 = y_2$, and that for a N^- reducing circle, $y_1 = y_2^{-1}$. \square

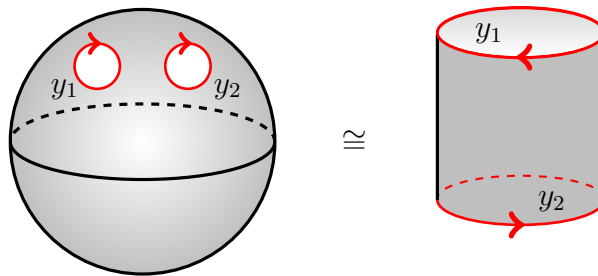


Figure 3.4: A continuous deformation of the twice punctured 2-sphere. We collapse all the 2-cell material by pushing in the boundary components y_1 and y_2 .

Note that we can read the relation $y_1 y_2^{-1} = 1$ or $y_1 y_2 = 1$ directly off the projection surface. To do so, we put an orientation on the reducing circle and use the “right hand rule” to read off the correct signs.

Lemma 3.2.2. *Given a virtual link diagram ℓ with a projection surface F , any simple closed curve that intersects ℓ n times gives a relation that holds in $\pi_1(D(\ell))$ under the map φ_* (from Equation 3.1).*

Proof. Suppose a simple closed curve on F intersects ℓ exactly n times at the edges y_1, y_2, \dots, y_n . We consider the edges, y_1, y_2, \dots, y_n , to be the (not necessarily distinct) generators of $\pi_1(W(\ell))$. Now proceed as we did in Proposition 3.2.1: look at the slice made by the simple closed curve on $\mathcal{M}(\ell)$. It is an annulus with n punctures, each puncture corresponding to a generator in the Wirtinger group. In the Dehn space, we cone off the top boundary of the slice and we cone off the bottom boundary of the slice. The result is a 2-sphere with n punctures, which is homeomorphic to a bouquet of $(n - 1)$ circles. We can determine the orientation of each generator if we place an orientation on the simple closed curve and use the “right hand rule” to read off the \pm orientation of each generator. We obtain a relation of the form: $y_1^{\epsilon_1} y_2^{\epsilon_2} \cdots y_n^{\epsilon_n} = 1$, for $\epsilon_i = \pm 1$. Moreover, $y_1^{\epsilon_1} y_2^{\epsilon_2} \cdots y_n^{\epsilon_n} = 1$ is in K , the kernel of $\varphi_* : \pi_1(W(\ell)) \rightarrow \pi_1(D(\ell))$. \square

Theorem 3.2.3 (Main Theorem I). *The fundamental group of the Dehn complex $\pi_1(D(\ell))$ is isomorphic to the quotient $\pi_1(W(\ell)) / K$ where K is normally generated by words $y_1^{\epsilon_1} y_2^{\epsilon_2} \cdots y_n^{\epsilon_n}$ that arise when reading along the curves that generate the fundamental group of the projection surface F .*

Proof. Recall from Definition 2.1.2 that the Dehn complex of a virtual link $D(\ell)$ is obtained by collapsing down the Dehn space $\mathcal{D}(\ell)$, ergo $\pi_1(\mathcal{D}(\ell)) \approx \pi_1(D(\ell))$. The Dehn space is obtained from the Wirtinger space by coning off the top surface, a projection surface F of ℓ . Denote C as this cone space, so that $\mathcal{D}(\ell) = \mathcal{W}(\ell) \cup C$. By considering a small open neighborhood of each $\mathcal{W}(\ell)$ and C , we can apply van

Kampen to this decomposition of $\mathcal{D}(\ell)$. Choose d_0 , the collapsible tree of $D(\ell)$, to be the basepoint. Affix d_0 to the decomposition of $\mathcal{D}(\ell)$.

$$\mathcal{D}(\ell) = (\mathcal{W}(\ell) \cup \{d_0\}) \cup (C \cup \{d_0\})$$

The basepoint d_0 collapses to the basepoint w_0 , since $w_0 \subset d_0$. Thus, $\pi_1(\mathcal{W}(\ell) \cup \{d_0\}, d_0)$ is isomorphic to $\pi_1(W(\ell), w_0)$. Every cone is contractible to its vertex point. Thus, $\pi_1(C \cup \{d_0\}, d_0)$ is isomorphic to $\{1\}$. As the intersection space $(\mathcal{W}(\ell) \cup \{d_0\}) \cap (C \cup \{d_0\})$ is homotopy equivalent to $F \cup \{d_0\}$, we consider the inclusion map $F \cup \{d_0\} \hookrightarrow (\mathcal{W}(\ell) \cup \{d_0\})$, which induces the homomorphism

$$i_* : \pi_1(F \cup \{d_0\}, d_0) \rightarrow \pi_1(W(\ell), w_0)$$

The fundamental group $\pi_1(F \cup \{d_0\}, d_0)$ is isomorphic to $\pi_1(F, x_0)$ for any basepoint x_0 on the projection surface, since d_0 is collapsible. Hence, the homomorphism i_* projects each generating curve of $\pi_1(F, x_0)$ to $\mathcal{W}(\ell)$. By Lemma 3.2.2, these curves give rise to words $y_1^{\epsilon_1} y_2^{\epsilon_2} \cdots y_n^{\epsilon_n}$, for $\epsilon_i = \pm 1$, that hold in $\pi_1(D(\ell))$. Therefore, K is generated as desired, and by van Kampen, $\pi_1(D(\ell))$ is isomorphic to $\pi_1(W(\ell)) / K$. \square

Example 3.2.4 (Virtual knot with finite $\pi_1(D(k))$). The alternating virtual knot diagram k in Figure 3.5 has Euler characteristic: $\chi = 3 - 6 + 3 = 0$. Hence, the projection surface of k is a torus. An orientation and appropriate labeling of the edges and connected components is shown in Figure 3.5. Therefore, we can write down the presentations of the Wirtinger group and of the Dehn group.

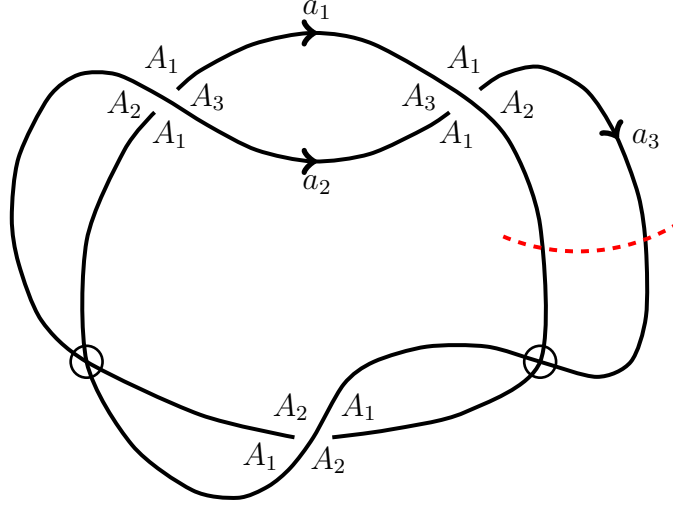


Figure 3.5: A fully labeled and oriented alternating virtual knot diagram with three crossings. The dashed red line represents a non-separating reducing circle. (Virtual knot number 3.7 from Green and Bar-Natan [6].)

$$\pi_1(W(k)) = \langle a_1, a_2, a_3 \mid a_2a_1 = a_1a_3, a_3a_2 = a_2a_1, a_2a_3 = a_3a_1 \rangle$$

$$\pi_1(D(k)) = \langle A_1, A_2, A_3 \mid A_1 = 1, A_1A_2^{-1}A_1A_3^{-1} = 1,$$

$$A_1A_2^{-1}A_1A_3^{-1} = 1,$$

$$A_1A_2^{-1}A_1A_2^{-1} = 1 \rangle$$

$$\approx \langle A_2, A_3 \mid A_3 = A_2^{-1}, A_2^2 = 1 \rangle$$

$$\approx \langle A_2 \mid A_2^2 = 1 \rangle$$

$$\approx \mathbb{Z}_2$$

In Harlander and Rosebrock [8], the Wirtinger group of this virtual knot was shown to have torsion.

A non-separating reducing circle is indicated in Figure 3.5. The reducing circle gives the relation $a_1 = a_3^{-1}$ in $\pi_1(D(k))$ under the surjective homomorphism φ_* (Proposition 3.2.1).

$$\begin{aligned}
\pi_1(W(k)) / \{a_1 = a_3^{-1}\} &\approx \langle a_3 | a_3^2 = 1 \rangle \\
&\approx \mathbb{Z}_2 \\
&\approx \pi_1(D(k))
\end{aligned}$$

Our conclusion is that when the groups are small, the number of generating curves necessary to obtain the Dehn group from the Wirtinger group may be less than as stated in Theorem 3.2.3.

3.3 Decomposition of the Dehn Complex

To obtain non-positive curvature in the Dehn complex—in light of Theorem 3.1.2— all reducing circles must be eliminated. We do this by cutting along the reducing circles and examining the affect on the fundamental group. An analog for classical knots of Theorem 3.3.1 can be found in Bridson and Haefliger [4].

Theorem 3.3.1. *Let ℓ be an alternating virtual link diagram with a projection surface F . If ℓ has a separating reducing circle on F which gives the composition $\ell = \ell_1 \# \ell_2$, then $\pi_1(D(\ell))$ is isomorphic to a quotient of a free product of alternating links*

$$\pi_1(D(\ell_1)) * \pi_1(D(\ell_2)) / N$$

where $N = \langle \langle A_i A_j^{-1} = A'_i A'_j^{-1} \rangle \rangle$. The reducing circle lies in the connected components, A_i and A_j , of F . We gain the connected components, A'_i and A'_j , when we cut along the reducing circle (see Figures 3.6 and 3.7).

Proof. By Lemma 2.4.4, ℓ_1 and ℓ_2 are alternating virtual link diagrams. We will use van Kampen to determine the fundamental group of $D(\ell)$ in terms of this composition

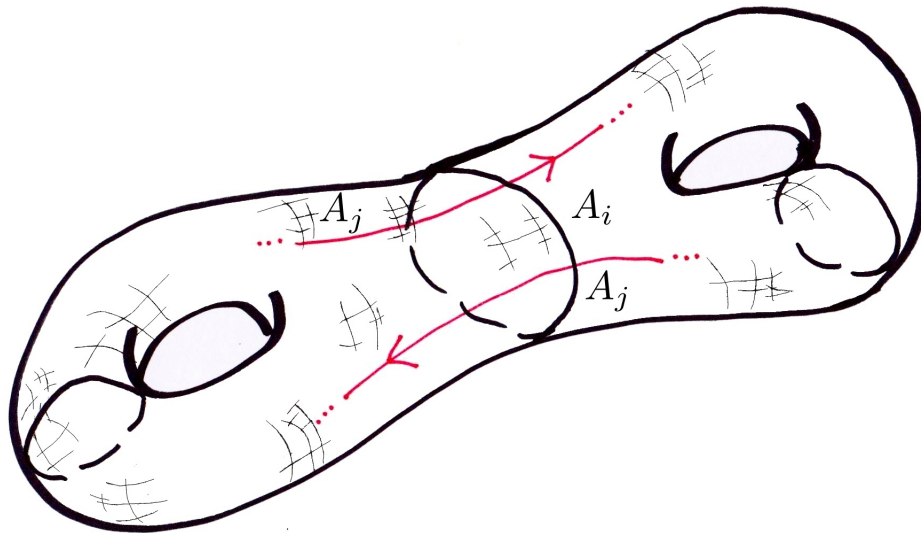


Figure 3.6: A double torus with a separating reducing circle indicated.

(see Hatcher [9]). Suppose the reducing circle cuts the edges y_1 and y_2 . Cut along the reducing circle, rendering $\mathcal{M}(\ell)$ into two pieces. The intersection of these pieces is an annulus A with two oriented punctures, y_1 and y_2 . Let the left-hand side be X_1 and the right-hand side be X_2 so that $\mathcal{M}(\ell) = X_1 \cup_A X_2$. This induces a decomposition of the Dehn space, $\mathcal{D}(\ell'_1) \cup_S \mathcal{D}(\ell'_2)$, where $S = \Sigma A$, and ΣA is A with the boundary circles coned off. The virtual link ℓ'_1 is the left-hand side of ℓ , and ℓ'_2 is the right-hand side of ℓ . The virtual link ℓ_1 is obtained from ℓ'_1 by gluing together the cut ends. In the same way, ℓ_2 is obtained from ℓ'_2 . Note that S is a twice-punctured 2-sphere and that y_1 and y_2 are the boundaries of those punctures. As shown in Proposition 3.2.1, $y_1 = y_2$ in $\pi_1(\mathcal{D}(\ell))$, and then also $y_1 = y_2$ in $\pi_1(\mathcal{D}(\ell'_i))$. Hence, $\pi_1(\mathcal{D}(\ell'_i)) = \pi_1(\mathcal{D}(\ell_i))$. Now van Kampen's theorem yields the decomposition of $\pi_1(\mathcal{D}(\ell))$,

$$\pi_1(\mathcal{D}(\ell_1)) * \pi_1(\mathcal{D}(\ell_2)) / \{y_1 = y_2\}$$

We can also express this in terms of the Dehn complexes rather than the Dehn

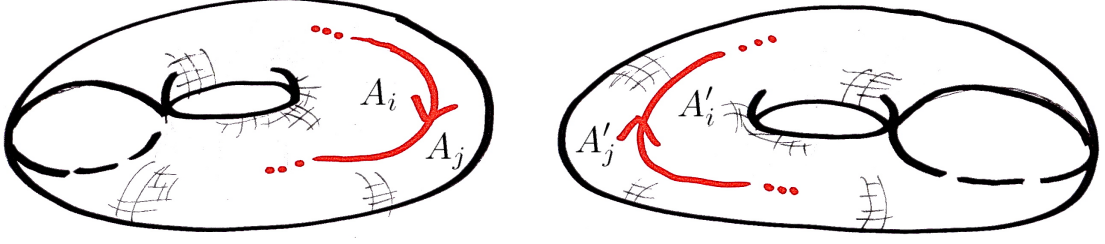


Figure 3.7: $\mathcal{M}(\ell_1)$ and $\mathcal{M}(\ell_2)$ obtained from $\mathcal{M}(\ell)$.

spaces. Note that in the Dehn complex $D(\ell_1)$, $y_1 = A_i A_j^{-1}$, and in the Dehn complex $D(\ell_2)$, $y_2 = A'_i A'_j^{-1}$ (see Figure 3.7). Hence, we have the decomposition of $\pi_1(D(\ell))$,

$$\pi_1(D(\ell_1)) * \pi_1(D(\ell_2)) / N$$

where $N = \langle\langle A_i A_j^{-1} = A'_i A'_j^{-1} \rangle\rangle$. If $\pi_1(D(\ell_1))$ and $\pi_1(D(\ell_2))$ are torsion free, it follows that $\pi_1(D(\ell))$ is an amalgamated free product, where $N \approx \mathbb{Z}$.

$$\pi_1(D(\ell)) = \pi_1(D(\ell_1)) *_N \pi_1(D(\ell_2))$$

□

A similar result may be obtained by induction for compositions of more than two alternating virtual link diagrams (Lemma 2.4.6).

Theorem 3.3.2. *Let ℓ be an alternating virtual link diagram with a projection surface F . If ℓ has a N^+ or N^- reducing circle on F , then $\pi_1(D(\ell))$ is a quotient of the alternating virtual link diagram ℓ' resulting from cutting the reducing circle*

$$\pi_1(D(\ell)) = \pi_1(D(\ell')) / \{A_i = A'_i, A_j = A'_j\}$$

where A_i and A_j are the connected components the reducing circle lies in on F , and A'_i and A'_j are the two components that we have gained by cutting the reducing circle, which cuts a handle in $\mathcal{M}(\ell)$.



Figure 3.8: A non-separating reducing circle on a handle of the projection surface of the virtual link ℓ and the resulting cut surface and virtual link ℓ' .

Proof. Recall from Definition 2.1.3 that the presentation of the Dehn group is of the form

$$\pi_1(D(\ell)) = \langle A_1, A_2, \dots, A_n \mid A_1 = 1, \quad A_{x(1)} A_{x(2)}^{-1} A_{x(3)} A_{x(4)}^{-1} = 1 \\ \text{for every crossing } x \in \ell \rangle$$

When we cut along a reducing circle in the Dehn complex, we do not add or take away any of the crossings of ℓ . However, we do add two new components, A'_i and A'_j , to the cut Dehn complex, $D(\ell')$ (see Figure 3.8). These two components will replace A_i or A_j , respectively, in some crossings of ℓ' . Therefore, we have the quotient

$$\pi_1(D(\ell)) = \pi_1(D(\ell')) / \{A_i = A'_i, A_j = A'_j\}$$

□

We now have fully described what happens to the fundamental group of the Dehn complex of a virtual link diagram when we cut along certain reducing circles.

Theorem 3.3.3 (Main Theorem II). *If ℓ is an alternating virtual link diagram drawn on a projection surface F , then we can cut along a finite number of reducing circles to obtain a collection of prime, alternating links, ℓ_1, \dots, ℓ_n . This gives a decomposition of the Dehn complex of ℓ , $D(\ell)$, into non-positively curved squared complexes, and a decomposition of the fundamental group of $D(\ell)$ into $CAT(0)$ groups.*

Proof. An alternating virtual link diagram ℓ with a projection surface F has a finite number of separating and non-separating reducing circles on F (Lemma 2.4.5). Theorem 3.3.1 shows how to cut along a single separating reducing circle and obtain a composition of links, $\ell = \ell_1 \# \ell_2$, and the free product

$$\pi_1(D(\ell)) = \pi_1(D(\ell_1)) * \pi_1(D(\ell_2)) / N$$

where N is explicitly defined. We may repeat this process for each separating reducing circle (Lemma 2.4.6).

Each piece, ℓ_i , of the composition of ℓ may have non-separating reducing circles. Theorem 3.3.2 shows how to cut along a single non-separating reducing circle to obtain an alternating virtual link, ℓ'_i , and the quotient

$$\pi_1(D(\ell_i)) = \pi_1(D(\ell'_i)) / \{A_i = A'_i, A_j = A'_j\}$$

Successive cuts would produce more connected components and further relations to record. Therefore, after cutting along every reducing circle, the resulting pieces will have non-positive curvature. □

3.4 Tripling a Virtual Knot

Reducing circles can be eliminated by sufficiently adding additional links to a virtual link diagram. One method is tripling a link. An alternating example of a tripled virtual knot diagram is shown in Figure 3.9.

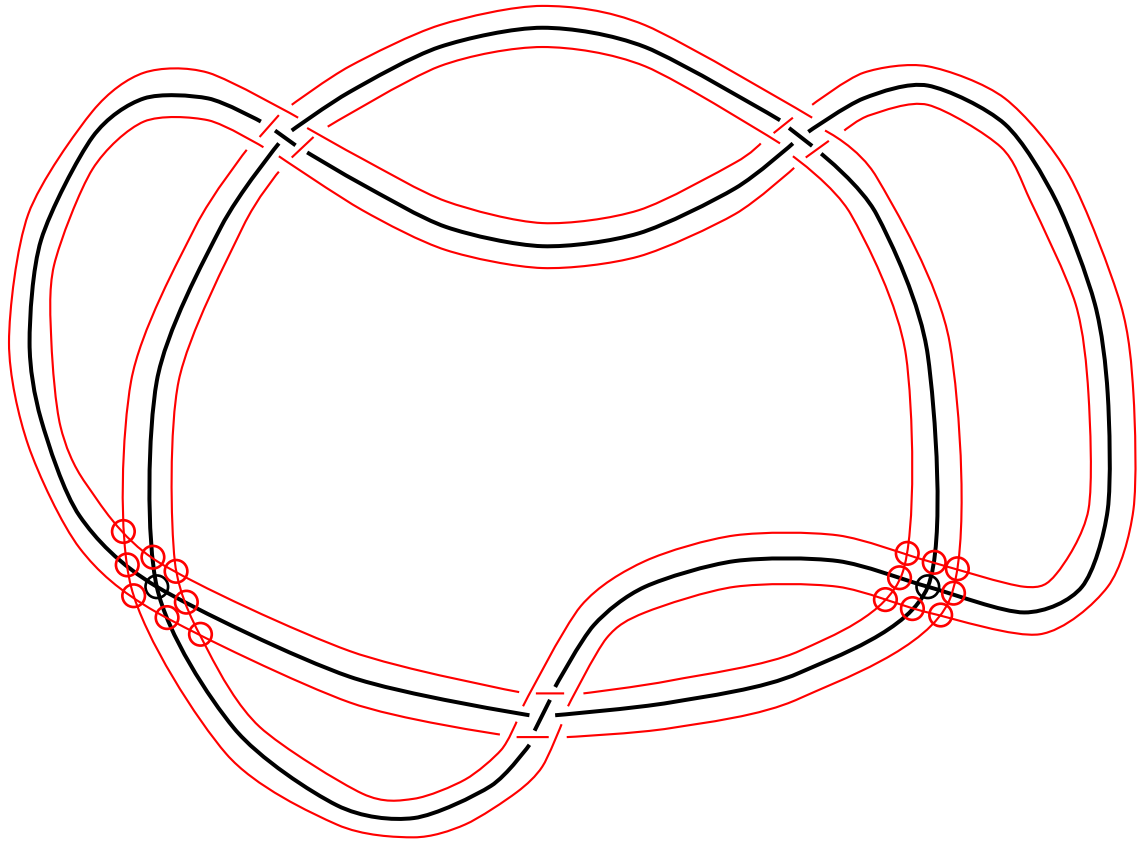


Figure 3.9: An alternating triple of an alternating virtual knot diagram (Example 3.2.4).

Definition 3.4.1. We triple a virtual link diagram ℓ by adding additional links, which run parallel on either side of all the original strands of the link. Denote the tripled link by ℓ_T .

Lemma 3.4.2. *There exists one triple of an alternating virtual link diagram that is alternating.*

Proof. After tripling an alternating virtual link diagram, ℓ , along every edge of ℓ there will be two additional crossings in between the original crossings of ℓ , which we may choose to alternate with the original crossings of ℓ (Figure 3.10). The only

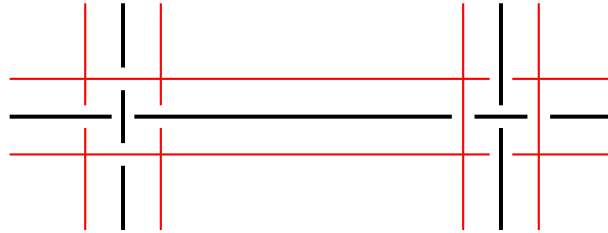


Figure 3.10: A portion of the alternating virtual link diagram ℓ (black strands) and the additional links from tripling ℓ (red strands). The new strands are chosen to alternate with the original strands.

remaining crossings we have not determined are those four crossings around each original crossing of ℓ made by the new links (the undetermined crossings in Figure 3.10). Immediately, these crossings may be chosen to alternate with the existing crossings (Figure 3.11), establishing that ℓ_T is alternating. \square

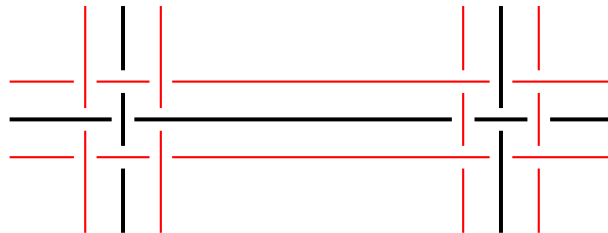


Figure 3.11: The remaining crossings of ℓ_T are chosen to alternate with the existing crossings.

Theorem 3.4.3. *If ℓ_T is an alternating triple of any alternating virtual link diagram ℓ , then $D(\ell_T)$ is a non-positively curved squared complex.*

Proof. Let ℓ_T be the triple of ℓ that is alternating (Lemma 3.4.2). If we can show ℓ_T is prime, Theorem 3.1.2 implies $D(\ell_T)$ is a non-positively curved squared complex. The virtual link ℓ_T is prime if there are no reducing circles (Definition 2.3.2).

We do not change the genus of the projection surface F when we triple ℓ . The new links are added to the existing projection surface. The original ℓ may have some reducing circles. When we triple ℓ , any previously existing reducing circle will become a closed curve that cuts the virtual link diagram in six places. A tripled link cannot form any additional reducing circles since every strand runs in sets of three between each square mesh of nine crossings. □

CHAPTER 4

VIRTUAL KNOT DIAGRAMS AND LABELED ORIENTED GRAPHS

4.1 Labeled Oriented Graphs

Definition 4.1.1. A Labeled Oriented Graph, shortened to LOG, is a finite graph with a finite set of vertices, say $\{a_1, a_2, \dots, a_n\}$. Each edge is oriented and labeled by one of the vertices. A Labeled Oriented Circle, shortened to LOC, is a LOG, where the graph forms a circle. Each edge in a LOG corresponds to a relation from which we can build a crossing, orienting the edges according to the “right hand rule,” as in Figure 4.1 (see Harlander and Rosebrock [7] and [8]).

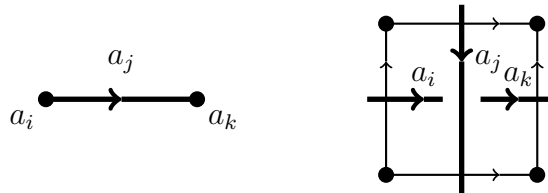


Figure 4.1: A single edge of a LOG and the knot diagram crossing associated to that edge. The edge of the LOG gives the Wirtinger relation $a_i a_j = a_j a_k$.

Every relation in the Wirtinger presentation corresponds to an oriented edge in a LOG with labeled vertices as shown in Figure 4.1. Since every edge in the virtual link must “start” and “end” in only two separate places, every edge occurs as a vertex in the LOG just once, with an edge “coming in” and another edge “going out.” It

follows that the LOG representing a virtual link diagram is a collection of LOCs. A virtual knot diagram would have a single representing LOC. In fact, we have shown the following proposition.

Proposition 4.1.2. *Every virtual link diagram can be represented by a collection of LOCs, whose edges give the relations of the Wirtinger presentation of the virtual link.*

Or, we may state that every virtual knot group can be represented by a LOC group (see Harlander and Rosebrock [8]).

If ℓ is an alternating virtual link diagram, every distinct edge corresponding to a generator of the Wirtinger group occurs once as an over-crossing, and thus occurs once as an oriented edge in the set of LOCs. If there are n distinct edges in the alternating virtual link, i.e. n distinct generators in the Wirtinger group, then there are n distinct edges and n distinct vertices in the corresponding set of LOCs labeled by the set of generators. We call such LOGs injective.

4.2 Virtual Knots with Trivial Dehn Group

We can determine when a virtual knot diagram k will have trivial $\pi_1(D(k))$ by the simple closed curves on a projection surface of k .

Proposition 4.2.1. *All generators in the canonical presentation of the Wirtinger group of a virtual knot diagram are conjugate to one another.*

Proof. For the virtual knot diagram k , there is a corresponding LOC that directly gives the relations of the Wirtinger group in terms of the generators, $\{a_1, \dots, a_n\}$, (Proposition 4.1.2). Each generator appears as a vertex in the LOC, though each generator may not appear as an edge in the LOC. We may choose the generator a_1 and show that a_1 is conjugate to the arbitrary generator a_i .

Starting at the vertex a_1 , we will proceed in a clockwise direction around our LOC, and we may assume a uniform orientation of the edges, since an opposite orientation of any one edge in the LOC would only change some $a_{jp} = a_{jp}^{-1}$ in the body of the proof. Let the vertex a_1 be connected to the vertex a_{k_1} by the edge a_{j_1} , which is given by the relation

$$\begin{aligned} a_1 a_{j_1} &= a_{j_1} a_{k_1} \\ a_1 &= a_{j_1} a_{k_1} a_{j_1}^{-1} \end{aligned}$$

Also let the vertex a_{k_1} be connected to the vertex a_{k_2} by the edge a_{j_2} , which is given by the relation

$$\begin{aligned} a_{k_1} a_{j_2} &= a_{j_2} a_{k_2} \\ a_{k_1} &= a_{j_2} a_{k_2} a_{j_2}^{-1} \\ &\vdots \end{aligned}$$

Continuing in this pattern, after some $m \leq n$ times, we will reach the vertex a_i on the LOC, giving us the relation

$$a_{k(m-1)} = a_{j_m} a_i a_{j_m}^{-1}$$

Therefore,

$$\begin{aligned} a_1 &= a_{j_1} a_{j_2} \cdots a_{j_m} a_i a_{j_m}^{-1} \cdots a_{j_2}^{-1} a_{j_1}^{-1} \\ &= (a_{j_1} a_{j_2} \cdots a_{j_m}) a_i (a_{j_1} a_{j_2} \cdots a_{j_m})^{-1} \end{aligned}$$

The generator a_1 is conjugate to the generator a_i . □

Corollary 4.2.2. *If a virtual knot diagram k with a projection surface F has a simple closed curve that intersects k on F only once, then $\pi_1(D(k)) = \{1\}$.*

Proof. This situation cannot occur for a classical knot with a projection surface of genus 0. We only consider virtual knot diagrams with a projection surface F of genus greater than or equal to 1.

Suppose that k has a simple closed curve that intersects the knot exactly once along the edge of k that corresponds to the Wirtinger generator a . By Lemma 3.2.2, this curve gives the relation $a = 1$, which holds in $\pi_1(D(k))$ under the surjective homomorphism φ_* (defined by Equation (3.1)). All the Wirtinger generators are conjugate (Proposition 4.2.1). Hence,

$$\begin{aligned} \pi_1(W(k)) / \{a = 1\} &\approx \{1\} \\ &\approx \pi_1(D(k)) \end{aligned}$$

□

Example 4.2.3 (Virtual knot with $\pi_1(D(k))$ trivial). In Example 2.1.5, we computed $\pi_1(D(k))$ by hand to find that it is trivial. Alternately, $\pi_1(D(k))$ is trivial by the presence of the simple closed curve that intersects k on the projection surface, a torus, exactly once. The presence of this curve also generates 1-cycles in the link graphs of k .

4.3 Examples of Decompositions of the Dehn Complex

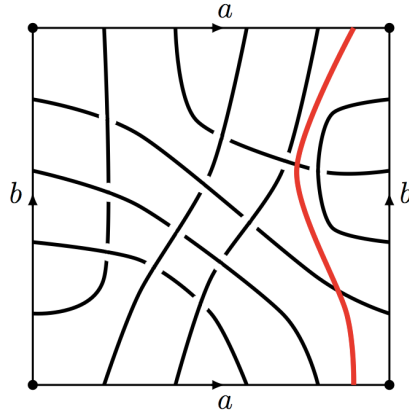


Figure 4.2: An alternating virtual knot diagram with one non-separating reducing circle, indicated by the red line, obtained by identifying the labeled edges.

Example 4.3.1 (Non-separating reducing circle on a torus). By identifying the indicated edges in Figure 4.2, we obtain an alternating virtual knot diagram on a torus. There is one non-separating reducing circle, thus the Dehn complex is not a non-positively curved squared complex. However, we may apply Theorem 3.3.3 to eliminate the reducing circle and obtain a Dehn complex that is a non-positively curved squared complex. By cutting along the indicated reducing circle in Figure 4.2, we cut the handle of the torus. The resulting prime knot lies on a 2-sphere (see Figure 4.3).

Example 4.3.2 (Non-separating reducing circles and separating reducing circles). The alternating virtual knot diagram k , in Figure 4.4, has Euler characteristic: $\chi = 4 - 8 + 4 = 0$. Hence, the projection surface of k is a torus.

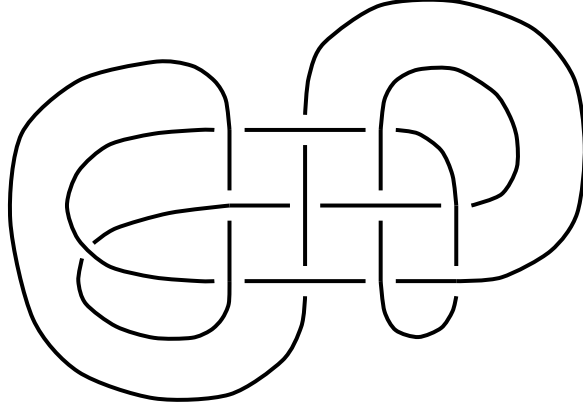


Figure 4.3: The alternating virtual link diagram of Figure 4.2 with the reducing circle cut out. The new prime knot is planar.

From the virtual knot diagram in Figure 4.4, we can write down the Dehn group.

$$\begin{aligned}
 \pi_1(D(k)) &= \langle A_1, A_2, A_3, A_4 \mid A_1 = 1, A_2 A_1^{-1} A_3 A_1^{-1} = 1, \\
 &\quad A_2 A_1^{-1} A_3 A_1^{-1} = 1, \\
 &\quad A_3 A_1^{-1} A_4 A_1^{-1} = 1, \\
 &\quad A_3 A_1^{-1} A_4 A_1^{-1} = 1 \rangle \\
 &\approx \langle A_2, A_3, A_4 \mid A_2 = A_3^{-1}, A_4 = A_3^{-1} \rangle \\
 &\approx \langle A_3 \rangle \\
 &\approx \mathbb{Z}
 \end{aligned}$$

In Figure 4.5, k has been cut and re-directed along the non-separating reducing circle indicated in Figure 4.4, resulting in the virtual knot k' . There are two new connected components, A'_1 and A'_3 , as shown.

This reducing circle we cut intersects the edges a_1 and a_4 in Figure 4.4. By Proposition 3.2.1, $a_1 = a_4$ in the Dehn group. Therefore, in the LOC, we identify the

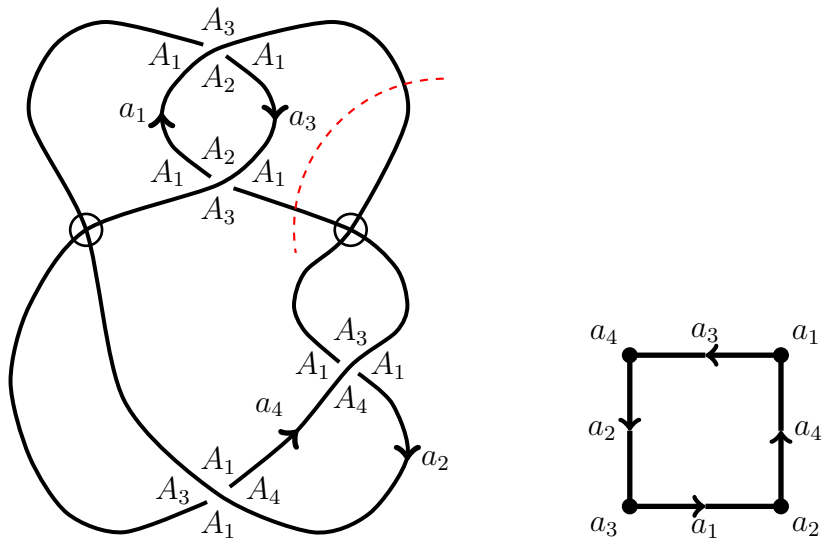


Figure 4.4: A labeled and oriented alternating virtual knot diagram with a non-separating reducing circle indicated by the red dashed line. On the right side is the corresponding LOC. (Virtual Knot number 4.105 from Green and Bar-Natan [6].)

vertices a_1 and a_4 . Then, we separate the LOG at the vertex $a_1 = a_4$ into two LOCs, thereby obtaining the LOCs of the virtual knot k' , as shown in Figure 4.5.

The fundamental group of the virtual knot k can be written as a quotient of the fundamental group of the virtual knot k' (Theorem 3.3.2),

$$\pi_1(D(k)) \approx \pi_1(D(k')) / \{A_1 = A'_1, A_3 = A'_3\}$$

where the Dehn group of k' is

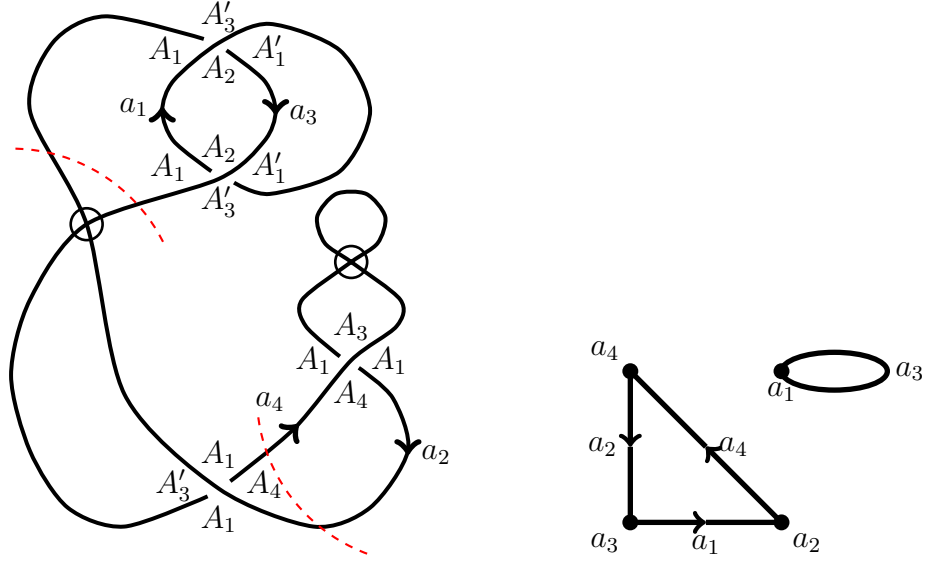


Figure 4.5: The resulting virtual knot diagram k' and its corresponding LOCs after cutting along the non-separating reducing circle indicated in Figure 4.4. The dashed red lines indicate separating reducing circles.

$$\begin{aligned}
 \pi_1(D(k')) &= \langle A_1, A_1', A_2, A_3, A_3', A_4 \mid A_1 = 1, A_2 A_1'^{-1} A_3 A_1^{-1} = 1, \\
 & \qquad \qquad \qquad A_2 A_1^{-1} A_3' A_1'^{-1} = 1, \\
 & \qquad \qquad \qquad A_3' A_1^{-1} A_4 A_1^{-1} = 1, \\
 & \qquad \qquad \qquad A_3 A_1^{-1} A_4 A_1^{-1} = 1 \rangle \\
 &\approx \langle A_2, A_3 \mid A_3 A_2 A_3^{-1} A_2^{-1} = 1 \rangle \\
 &\approx \mathbb{Z} \times \mathbb{Z}
 \end{aligned}$$

The projection surface of k' is a 2-sphere. However, there are still reducing circles present in the virtual knot diagram. Cutting along the two separating reducing circles indicated in Figure 4.5 results in three prime virtual links, k'_1 , k'_2 and k'_3 , as shown in Figure 4.6, which have non-positive curvature.

Using Theorem 3.3.2 and Theorem 3.3.1, we can find the fundamental group of k

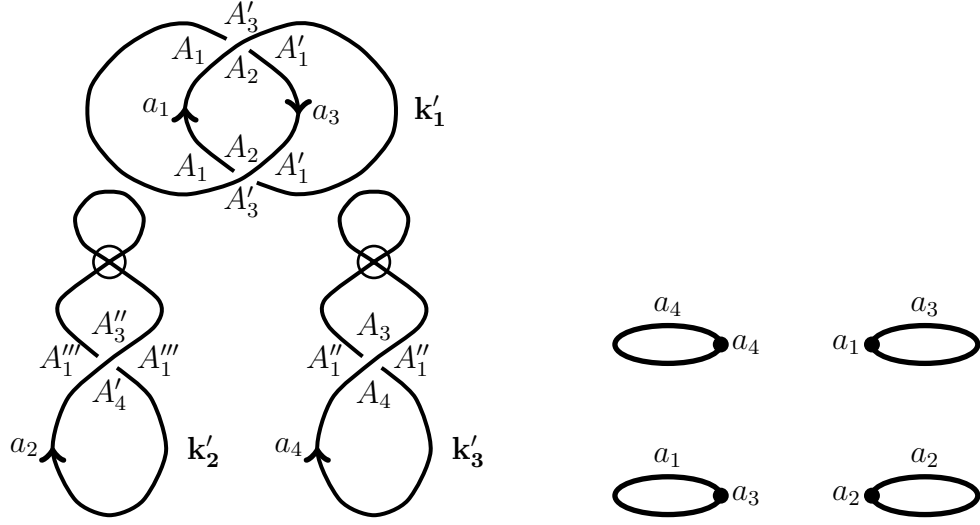


Figure 4.6: The resulting virtual link diagram of k'_1 , k'_2 , and k'_3 and their corresponding LOCs after cutting along the separating reducing circles indicated in Figure 4.5.

in terms of k'_1 , k'_2 , and k'_3 . First, we find the Dehn groups of k'_1 , k'_2 and k'_3 .

$$\begin{aligned} \pi_1(D(k'_1)) &= \langle A_1, A'_1, A_2, A'_3 \mid A_1 = 1, A_2 A_1^{-1} A'_3 A_1^{-1} = 1, A_2 A_1^{-1} A'_3 A_1^{-1} = 1, \rangle \\ &\approx \mathbb{Z} \times \mathbb{Z} \\ \pi_1(D(k'_2)) &= \langle A'''_1, A''_3, A'_4 \mid A'''_1 = 1, A''_3 A'''_1^{-1} A'_4 A'''_1^{-1} = 1 \rangle \\ &\approx \mathbb{Z} \\ \pi_1(D(k'_3)) &= \langle A''_1, A_3, A_4 \mid A''_1 = 1, A_3 A''_1^{-1} A_4 A''_1^{-1} = 1 \rangle \\ &\approx \mathbb{Z} \end{aligned}$$

In this case, the virtual knot k' can be written as an amalgamated product of the fundamental groups of k'_1 , k'_2 , and k'_3 , where the normal subgroups are obtained as described in Theorem 3.3.1.

$$\begin{aligned}\pi_1(D(k')) &\approx \pi_1(D(k'_1)) *_{N_1} \pi_1(D(k'_2)) *_{N_2} \pi_1(D(k'_3)) \\ N_1 &= \langle A_1 A'_3{}^{-1} = A''_1 A''_3{}^{-1} \rangle \\ N_2 &= \langle A'_4 A''_1{}^{-1} = A_4 A''_1{}^{-1} \rangle\end{aligned}$$

Note that instead of making further cuts on k' , we could have used Type I Reidemeister moves, for planar and virtual knots (Kauffman [13]), to obtain a link with the same fundamental group. The additional knots, k'_2 and k'_3 , we obtained are equivalent to the unknot. Moreover, it is easy to verify that $\pi_1(D(k')) \approx \pi_1(D(k'_1)) \approx \mathbb{Z} \times \mathbb{Z}$. Therefore, we can express the fundamental group of the Dehn complex of k in several ways,

$$\begin{aligned}\pi_1(D(k)) &\approx \pi_1(D(k'_1)) *_{N_1} \pi_1(D(k'_2)) *_{N_2} \pi_1(D(k'_3)) / \{A_1 = A'_1, A_3 = A'_3\} \\ &\approx \pi_1(D(k')) / \{A_1 = A'_1, A_3 = A'_3\}\end{aligned}$$

Further examples of virtual knot diagrams can be found online from Green Bar-Natan [6] or can be produced on a surface as Figure 3.1 and Figure 4.2.

CHAPTER 5

ASPHERICITY OF VIRTUAL KNOTS

In this chapter, we attempt to provide a summary of the results surrounding my thesis topic and illustrate how my results fit into the overall picture.

The following conjecture has remained open in spite of intense work from various approaches. Originally motivated by determining whether classical knot complements were aspherical, the range of the conjecture has broadened considerably since then.

Is any subcomplex of an aspherical, 2-dimensional complex itself aspherical?

–J. H. C. Whitehead (1941) [17]

A connected 2-dimensional CW complex X is aspherical if $\pi_2(X)$ is the trivial group. The classical knot complement—a knot k removed from a 3-sphere—is a 3-manifold with boundary, and hence has the homotopy type of a 2-complex. If we add a meridional disc to the knot complement, we obtain a 3-sphere with a ball removed, which is itself a ball. Thus, the classical knot complement is homotopic to a 2-complex that embeds in a contractible 2-complex. Knot complements have since been shown to be aspherical (Papakyriakopoulos [14]). For a complete overview of the work done on the Whitehead conjecture, see Rosebrock [15] and Bogley [3].

With the introduction of virtual knots, there is the new question of whether virtual knot complements are aspherical. For a virtual knot diagram k with a projection

surface F , Definition 2.1.2 described three distinct knot complements—the manifold space $\mathcal{M}(k)$, the Wirtinger space $\mathcal{W}(k)$, and the Dehn space $\mathcal{D}(k)$. We now consider asphericity in regards to these various knot complements.

5.1 Classical Closed Knot

The projection surface of the classical closed knot is the 2-sphere. The manifold space, which is $S^2 \times I - k$, and the Wirtinger space, which is $B^3 - k$, are clearly not aspherical because they admit non-trivial boundary spheres. However, the Dehn space, which is $S^3 - k$, has been shown to be aspherical.

When the Dehn complex of a classical knot is a non-positively curved squared complex, then the complex is also diagrammatically reducible (Gersten [5]). Every spherical diagram of a diagrammatically reducible complex is reducible, thus the complex is combinatorially aspherical, which implies topological asphericity.

5.2 Virtual Closed Knot

When the projection surface of a closed knot is not the 2-sphere—strictly the virtual case—the results on asphericity change dramatically. The manifold space is now, $F \times I - k$, an orientable 3-manifold with boundary. We can use 3-manifold techniques, just like in the classical case, to show that $\mathcal{M}(k)$ is aspherical.

The Wirtinger space and the Dehn space of a virtual knot need not be aspherical. The virtual knot given in Example 3.2.4 has a Wirtinger group and a Dehn group with torsion, hence the Wirtinger space and the Dehn space of the virtual knot are not aspherical.

In this thesis, we studied the geometry of the 2-dimensional spine of $\mathcal{D}(k)$. In attempting to adapt results of non-positive curvature for classical knots to virtual knots, we have had to grapple with the consequence of looking at knots on surfaces of higher genus. The existence of reducing circles that only cut a handle, rather than separate the surface, create circumstances that are non-existent in the classical knot world, as we have explored in this thesis. The results of Theorem 3.3.3 allow us to eliminate the separating *and* the non-separating reducing circles and thereby obtain non-positively curved pieces, having recorded the damage done to the fundamental group of the original complex.

5.3 Virtual Long Knot

A virtual long knot is a collection of “knotted” arcs properly embedded in a fattened projection surface with boundary, such that the endpoints of the embedded arcs lie on the boundary of the surface.

In the case of a classical long knot, the complements $\mathcal{M}(k)$, $\mathcal{W}(k)$, and $\mathcal{D}(k)$ all agree. In particular, they are all aspherical.

The manifold space of a virtual long knot is aspherical by 3-manifold techniques.

The results of this thesis may be applied to virtual long knots. The Dehn space need not be aspherical for virtual long knots since $\pi_1(\mathcal{D}) \approx \pi_1(\hat{\mathcal{D}})$, where $\hat{\mathcal{D}}$ is the Dehn space of the associated closed knot.

If we limit ourselves to alternating long virtual knots with no non-separating reducing circles, then Harlander and Rosebrock [7] have shown that if the Dehn complex of a long virtual knot, with $\text{genus}(F) \geq 1$, is diagrammatically reducible, then the Wirtinger complex is aspherical. Moreover, Harlander and Rosebrock [7]

also gave a “gluing lemma,” such that we may cut an alternating virtual knot along its separating reducing circles, and then glue the pieces back together in such a way that the result is diagrammatically reducible. Hence, we have the asphericity of the Wirtinger complex.

It is still an open question whether the Wirtinger space of every virtual long knot—more generally, every labelled oriented tree—is aspherical.

REFERENCES

- [1] C. C. Adams. *The Knot Book: an Elementary Introduction to the Mathematical Theory of Knots*. W. H. Freeman and Company, New York, 1994.
- [2] R. J. Aumann. Asphericity of alternating knots. *Annals of Mathematics*, 64(2):374–392, 1956.
- [3] W. A. Bogley. J. H. C. Whitehead’s asphericity question. In A. Sieradski C. Hog-Angeloni and W. Metzler, editors, *Two-dimensional Homotopy and Combinatorial Group Theory*, volume 197 of *LMS Lecture Notes*, pages 309–334. Cambridge University Press, 1993.
- [4] M. R. Bridson and A. Haefliger. *Metric Spaces of Non-Positive Curvature*. Springer, Berlin, 1999.
- [5] S. M. Gersten. Reducible diagrams and equations over groups. In *Essays in Group Theory*, volume 8. Mathematical Science Research Institute Publications, Springer Verlag, 1987.
- [6] J. Green and D. Bar-Natan. A table of virtual knots. <http://www.math.toronto.edu/~drorbn/Students/GreenJ/>, August 2004. Accessed: June 15, 2011.
- [7] J. Harlander and S. Rosebrock. Generalized knot complements and some aspherical ribbon disc complements. *J. of Knot Theory and Its Ramifications*, 12(7):947–962, 2003.
- [8] J. Harlander and S. Rosebrock. On distinguishing virtual knot groups from knot groups. *J. of Knot Theory and Its Ramifications*, 19(5):695–704, 2010.
- [9] A. Hatcher. *Algebraic Topology*. Cambridge University Press, 2001.
- [10] C. Hog-Angeloni and W. Metzler. Geometric aspects of 2-dimensional complexes. In A. Sieradski C. Hog-Angeloni and W. Metzler, editors, *Two-dimensional Homotopy and Combinatorial Group Theory*, volume 197 of *LMS Lecture Notes*, pages 189–218. Cambridge University Press, 1993.

- [11] N. Kamada. On the Jones polynomials of checkerboard colorable virtual links. *Osaka J. Mathematics*, 39:325–333, 2002.
- [12] L. H. Kauffman. Introduction to virtual knot theory. <http://arxiv.org/abs/1101.0665>, 2011. Submitted.
- [13] L.H. Kauffman. Virtual knot theory. *Europ. J. Combinatorics*, 20:663–691, 1999.
- [14] C. D. Papakyriakopoulos. On Dehn’s lemma and the asphericity of knots. *Annals of Mathematics*, 66:1–26, 1957.
- [15] S. Rosebrock. The Whitehead conjecture - an overview. *Siberian Electronic Mathematical Reports*, 4:440–449, 2007.
- [16] C. M. Weinbaum. The word and conjugacy problems for the knot group of any tame prime alternating knot. *Proc. American Mathematical Society*, 30:22–26, 1971.
- [17] J. H. C. Whitehead. On adding relations to homotopy groups. *Annals of Mathematics*, 42:409–428, 1941.
- [18] D. T. Wise. *Non-positively curved squared complexes, aperiodic tilings, and non-residually finite groups*. PhD thesis, Princeton University, 1996.